

# Graviton-photon production with a massive spin-2 particle

Joshua A. Gill, Dipan Sengupta, and Anthony G. Williams

*ARC Centre of Excellence for Dark Matter Particle Physics,*

*Department of Physics, University of Adelaide, South Australia 5005, Australia*

A recent letter [1] within a phenomenological dark matter framework with a massive graviton in the external state indicated a divergence with increasing centre-of-momentum energy arising from the longitudinal polarizations of the graviton. In this letter we point out that in processes such as graviton-photon production from matter annihilation,  $f\bar{f} \rightarrow G\gamma$ , no such anomalous divergences occur at tree-level. This then applies to other tree-level amplitudes related by crossing symmetry such as  $\gamma f \rightarrow Gf$ ,  $Gf \rightarrow \gamma f$ ,  $\gamma\bar{f} \rightarrow G\bar{f}$ ,  $f \rightarrow fG\gamma$  and so on. We show this by explicitly computing the relevant tree-level diagrams, where we find that delicate cancellations ensure that all anomalously growing terms are well-regulated. Effectively at tree-level this is consistent with the operation of a Ward identity associated with the external photon for such amplitudes. The same tree-level results apply if the photon is replaced by a gluon. These results are important for cosmological models of dark matter within the framework of extra dimensions.

## I. INTRODUCTION

In the last few years, there has been a renewed interest in dark matter and phenomenological models with massive spin-2 particles [1–3]. While some of these approaches are simplified constructions of an underlying compact extra-dimensional theory [4], others are effective field theories with a single massive graviton [5]. In a number of these approaches, it has been shown that there are enhancements in matrix elements and cross-sections due to the longitudinal polarizations of the graviton, which grow like  $\mathcal{O}(s/M_G^2)$  at high energies, where  $s$  is the centre-of-momentum energy and  $M_G$  the mass of the massive spin-2 particle [1, 2, 5]. These require a lower bound on the graviton mass  $M_G$  in order for the theory to be effective at large  $s^1$ . This high energy scaling is expected in a naive Fierz-Pauli theory [8] or extensions like bigravity/dRGT gravity [9–11]<sup>2</sup>. However, in Kaluza-Klein (KK) theories with compact extra dimensions [12–14], spin-2 KK mode scatterings are unitarized due to the underlying higher dimensional diffeomorphism invariance [15–17]<sup>3</sup>. In KK theories, these results have been extended to coupling with matter localized on the four-dimensional brane [20].

In a recent letter [1], the authors have pointed out that in a simple graviton-gluon production process,  $f\bar{f} \rightarrow Gg$ , with a gluon and a massive spin-2 particle in the external state, there is a chiral-symmetry-breaking enhancement due to a massive on-shell external fermion. They found

that the squared matrix elements for the longitudinal polarizations grow proportional to  $\left[(s/M_{Pl}^2)\left(m_f^4/M_G^4\right)\right]$  at high energies, implying an increase with increasing fermion mass  $m_f$  and a very strong enhancement with decreasing graviton mass,  $M_G \rightarrow 0$ . This should be compared with a growth of the form  $|\mathcal{M}|^2 \propto \mathcal{O}(s/M_{Pl}^2) < 1$  for a massless graviton theory since theories involving gravitons are effective field theories which are valid for  $s \ll M_{Pl}$ . In Ref. [1] this enhanced result was then used to estimate the relic density in a freeze-in dark matter model with a cosmologically stable light KK graviton. This model then showed a dramatic enhancement in the velocity averaged cross-section for  $M_G \ll m_f$ .

The result also implies that even in a compactified extra-dimensional setup with massive KK modes in the external state, this enhancement should persist even when the full KK spectrum is taken into account, since there is no cancellation mechanism, in contrast to expectations of scaling of KK graviton scatterings respecting higher dimensional gauge/diffeomorphism invariance. The enhancement also has significant phenomenological consequences for the production of KK gravitons at high-energy colliders within extra-dimensional models, which would predict anomalously growing cross-sections for fermion-initiated processes.

In this letter, we explicitly calculate the graviton-photon production process<sup>4</sup>,

$$f\bar{f} \rightarrow G\gamma, \quad (1)$$

where  $G$  represents a massive spin-2 particle<sup>5</sup>, and  $\gamma$  the massless on-shell photon. We show that the full tree-level squared amplitude at high energies grows as  $|\mathcal{M}|^2 \propto \mathcal{O}(s/M_{Pl}^2)$ , and there are no terms proportional to  $m_f^4/M_G^4$ , implying no enhancements or divergences as

<sup>1</sup>The  $M_G \rightarrow 0$  limit is not smooth and leads to the famous vanDam-Veltman-Zakharov discontinuity [6, 7].

<sup>2</sup>At high energies the scattering amplitudes of massive gravitons ( $GG \rightarrow GG$ ) in the Fierz-Pauli theory grows as  $s^5/(M_G^8 M_{Pl}^2)$ , which can be estimated from power counting arguments [10, 11]. It can be shown that in extensions like dRGT gravity, this scaling can be improved to  $s^3/(M_G^4 M_{Pl}^2)$  by adding higher order terms in the potential, but not beyond [9].

<sup>3</sup>It can be shown through a rigorous calculation that these cancellations persist even when the radial mode, the radion, gets a mass via the Goldberger-Wise mechanism [18, 19].

<sup>4</sup>Graviton photoproduction  $\gamma f \rightarrow Gf$  has been calculated previously in [21] for massless gravitons.

<sup>5</sup>This can be either a massive spin-2 particle in theories of massive gravity, or a massive spin-2 KK graviton.

$M_G \rightarrow 0$  for finite fermion masses, contrary to the suggestion in [1]. We demonstrate that although individual terms in the  $s$ ,  $t$ ,  $u$  and contact interactions grow as  $\mathcal{O}(1/M_G^2)$ , due to the longitudinal polarizations of the massive graviton, delicate cancellations at tree-level ensure that the full amplitude has no low energy cut-off, for all incoming helicities of the fermion and outgoing helicities of the massless photon and the massive graviton. An identical scaling of amplitudes at high energies is observed if a gluon replaces the photon. The only difference is replacing the electromagnetic coupling with the strong coupling. In the following sections, we detail the calculation and present the full amplitude as a function of the centre-of-momentum energy  $s$  and scattering angle  $\theta$ .

## II. FRAMEWORK AND FORMALISM

We use the ‘mostly minus’ metric convention for the flat four-dimensional Minkowski spacetime background (4D)  $\eta_{\mu\nu} \equiv \text{Diag}(+1, -1, -1, -1)$ , which is also used to raise and lower indices. Metric fluctuations  $h_{\mu\nu}(x)$ <sup>6</sup> around the flat Minkowski background is expressed as,

$$\eta_{\mu\nu} \rightarrow \eta_{\mu\nu} + \kappa h_{\mu\nu}(x) \equiv \tilde{G}_{\mu\nu}(x), \quad (2)$$

which define the spin-2 graviton in 4D. The dimensionfull coupling  $\kappa$  is related to the fundamental 4D Planck mass as  $\kappa = 1/M_{Pl} = \sqrt{16\pi G_N}$ . A theory of massive graviton, dubbed as the Fierz-Pauli theory, can be expressed as,

$$\mathcal{L} = \frac{M_{Pl}^2}{2} \sqrt{-|\tilde{G}|} R + \frac{M_G^2}{2} (h^2 - h_{\mu\nu}^2). \quad (3)$$

Here  $|\tilde{G}|$  is the determinant of 4D metric with fluctuations and  $h \equiv \eta^{\mu\nu} h_{\mu\nu}$ . The first term represents the Einstein-Hilbert piece,  $R$  being the Ricci scalar, while the second represents the Fierz-Pauli mass term. In theories of compact extra dimensions, the same mass terms for spin-2 KK gravitons appear after compactification, along with the massless graviton. For example, in Randall-Sundrum models in warped extra dimensions, the masses of the  $n^{th}$  modes of the spin-2 KK gravitons are given by (in the large curvature limit)  $m_n \simeq x_n k e^{-\pi k r_c}$ , where  $x_n$  are the zeros of the Bessel function of the first kind,  $k$  is the curvature and  $r_c$  the radius of the compactification.

The couplings of the graviton to matter (scalars, fermions or vectors) can be expressed by the following action,

$$\mathcal{S}_M = \int d^4x \mathcal{L}(\tilde{G}, s, v, f), \quad (4)$$

which upon expanding to order  $\kappa$  in the metric fluctuation yields,

$$\mathcal{S}_M = -\frac{\kappa}{2} \int d^4x h_{\mu\nu} T^{\mu\nu}(s, v, f). \quad (5)$$

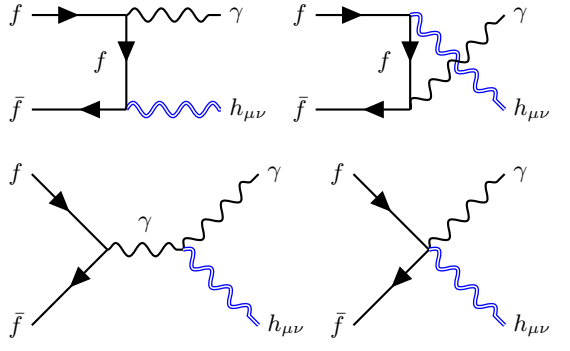


FIG. 1. Feynman diagrams for the process  $f(p_1) + \bar{f}(p_2) \rightarrow \gamma(k_1) + G(k_2)$

The stress energy tensor  $T_{\mu\nu}$  is given by,

$$T_{\mu\nu} = \left( -\eta_{\mu\nu} \mathcal{L} + 2 \frac{\delta \mathcal{L}}{\delta \tilde{G}^{\mu\nu}} \right) |_{\tilde{G}=\eta}. \quad (6)$$

For fermions, the stress-energy tensor must be calculated using the Vielbein formalism as performed in [12, 22]. We follow [12, 22] for the conventions and Feynman rules. The process of interest here is graviton-photon production via the annihilation of a fermion and anti-fermion pair, as expressed in Eq. 1. The four diagrams shown in Fig. 1,  $t$ -,  $u$ -,  $s$ -channels and a contact term, respectively, are the only tree-level interactions. The vertex rules are derived in [12] and are listed in the supplementary material. The coupling between the fermion and the photon is  $g_{fe}$ , where  $e \equiv |e|$  is the magnitude of the charge of the electron. The coupling between the fermions and the graviton is  $\kappa = 1/M_{Pl}$ .

We define the following variable, which will appear in the  $s$ -channel diagram with a gauge parameter  $\xi$ , as:

$$\begin{aligned} W_{\mu\nu\alpha\beta}(k_1, k_2; \xi) = & (1/2) \eta_{\mu\nu} (k_{1\beta} k_{2\alpha} - k_1 \cdot k_2 \eta_{\alpha\beta}) \\ & + \eta_{\mu\alpha} (k_1 \cdot k_2 \eta_{\nu\beta} - k_{1\beta} k_{2\nu}) \\ & + \eta_{\alpha\beta} k_{1\mu} k_{2\nu} - \eta_{\mu\beta} k_{1\nu} k_{2\alpha} \\ & - (1/\xi) \{ (\eta_{\nu\beta} k_{1\mu} k_{1\alpha} + \eta_{\nu\alpha} k_{2\mu} k_{2\beta}) \\ & - (1/2) \eta_{\mu\nu} (k_{1\alpha} k_{1\beta} + k_{2\alpha} k_{2\beta} + k_{1\alpha} k_{2\beta}) \}. \end{aligned} \quad (7)$$

The photon propagator is defined as,

$$\Delta_{\mu\nu}(Q) = -\frac{i}{Q^2} \left[ \eta_{\mu\nu} + (\xi - 1) \frac{Q_\mu Q_\nu}{Q^2} \right]. \quad (8)$$

For simplicity, we work in Feynman gauge  $\xi = 1$ . The fermion propagator with momentum  $Q$  and mass  $m_f$  travelling in the direction of the fermion flow is given by,

$$S_F(Q) = \frac{i(\not{Q} + m_f)}{Q^2 - m_f^2}. \quad (9)$$

<sup>6</sup>From here on we will drop the spacetime index  $x$ , and in momentum space  $k$  unless explicitly specified.

We define the Mandelstam variables such that,

$$s = (p_1 + p_2)^2 = (k_1 + k_2)^2, \quad (10)$$

$$t = (p_1 - k_1)^2 = (p_2 - k_2)^2, \quad (11)$$

$$u = (p_1 - k_2)^2 = (p_2 - k_1)^2. \quad (12)$$

Choosing the  $\hat{z}$  direction as the centre-of-momentum frame, with an outgoing massless photon and a massive graviton with mass  $M_G$ , we can express the four-momenta of various particles as,

$$p_1^\mu = (E_{p_1}, |\mathbf{p}| \hat{z}), \quad p_1^2 = m_f^2, \quad (13)$$

$$p_2^\mu = (E_{p_2}, -|\mathbf{p}| \hat{z}), \quad p_2^2 = m_f^2, \quad (14)$$

$$k_1^\mu = E_{k_1} (1, -\hat{k}), \quad k_1^2 = 0, \quad (15)$$

$$k_2^\mu = (E_{k_2}, \mathbf{k}), \quad k_2^2 = M_G^2. \quad (16)$$

The momentum ( $\mathbf{k}$ ) of the outgoing graviton and photon are given in terms of the inclination and azimuthal angle pairing  $(\theta, \phi)$  as  $\mathbf{k} = |\mathbf{k}|(s_\theta c_\phi, s_\theta s_\phi, c_\theta)$ , where  $c_\theta \equiv \cos \theta$  and  $s_\theta \equiv \sin \theta$ . The polarizations for the external on-shell photon are defined in the usual way,

$$\varepsilon_{\pm 1}^\mu(k_1) = \pm \frac{e^{\pm i\phi}}{\sqrt{2}} \left( 0, -c_\theta c_\phi \pm i s_\phi, -c_\theta s_\phi \mp i c_\phi, s_\theta \right). \quad (17)$$

A helicity- $\lambda_G$  massive graviton carries five polarizations  $\varepsilon_{\lambda_G}^{\mu\nu}(k)$ . These are grouped into two transverse, and three longitudinal polarizations, which can be split into two helicity-1 modes and one helicity-0 mode, defined respectively as [15],

$$\lambda_G = \pm 2, \quad \varepsilon_{\pm 2}^{\mu\nu} = \varepsilon_{\pm 1}^\mu \varepsilon_{\pm 1}^\nu, \quad (18)$$

$$\lambda_G = \pm 1, \quad \varepsilon_{\pm 1}^{\mu\nu} = \frac{1}{\sqrt{2}} \left[ \varepsilon_{\pm 1}^\mu \varepsilon_0^\nu + \varepsilon_0^\mu \varepsilon_{\pm 1}^\nu \right], \quad (19)$$

$$\lambda_G = 0, \quad \varepsilon_0^{\mu\nu} = \frac{1}{\sqrt{6}} \left[ \varepsilon_{+1}^\mu \varepsilon_{-1}^\nu + \varepsilon_{-1}^\mu \varepsilon_{+1}^\nu + 2 \varepsilon_0^\mu \varepsilon_0^\nu \right], \quad (20)$$

where  $\varepsilon_{\pm 1}^\mu$  are the usual polarization vectors for the photon defined in Eq. 17, while the helicity-0 polarization is defined by,

$$\varepsilon_0^\mu(k_2) = \frac{E_{k_2}}{M_G} \left( \sqrt{1 - \frac{M_G^2}{E_{k_2}^2}}, \hat{k} \right). \quad (21)$$

The polarization vectors for momentum  $k_2$  are defined using the same angle pairs  $(\theta, \phi)$ . Without loss of generality, we have chosen  $\phi = 0$  in the calculation.

Choosing the centre-of-momentum frame for the incoming particles with four-vectors  $p_1$  and  $p_2$ , and outgoing four-vectors  $k_1$  and  $k_2$ , the outgoing energies  $E_{k_1}$  and  $E_{k_2}$  can be expressed in terms of the Mandelstam variable  $s$  and the mass of the graviton  $M_G$  as,

$$E_{k_1} = \frac{s - M_G^2}{2\sqrt{s}}, \quad E_{k_2} = \frac{s + M_G^2}{2\sqrt{s}}. \quad (22)$$

For the Feynman diagrams depicted in Fig. 1, with an incoming fermion  $f(p_1)$  and anti-fermion  $\bar{f}(p_2)$  scattering to a photon with polarization  $\varepsilon_\lambda(k_1)$  and a massive graviton with polarization  $\varepsilon_{\lambda_G}^{\mu\nu}$ , the matrix elements<sup>7</sup> for the  $t$ ,  $u$ ,  $s$  and the contact diagrams are respectively given by,

$$\mathcal{M}_t = -\frac{\kappa g_f e}{4} \bar{v}_{\lambda_1}(p_2) [\gamma_\mu P_\nu + \gamma_\nu P_\mu - 2\eta_{\mu\nu} (\not{P} - 2m_f)] \times \left( \frac{\not{p}_1 - \not{k}_1 + m_f}{t - m_f^2} \right) \not{v}_{\lambda_\gamma}^*(k_1) \varepsilon_{\lambda_G}^{*\mu\nu}(k_2) u_{\lambda_2}(p_1), \quad (23)$$

$$\mathcal{M}_u = -\frac{\kappa g_f e}{4} \bar{v}_{\lambda_1}(p_2) \not{v}_{\lambda_\gamma}^*(k_1) \left( \frac{\not{p}_1 - \not{k}_2 + m_f}{u - m_f^2} \right) \times [\gamma_\mu K_\nu + \gamma_\nu K_\mu - 2\eta_{\mu\nu} (\not{K} - 2m_f)] \varepsilon_{\lambda_G}^{*\mu\nu}(k_2) u_{\lambda_2}(p_1), \quad (24)$$

$$\mathcal{M}_s = \frac{\kappa g_f e}{s} \bar{v}_{\lambda_1}(p_2) \gamma^\alpha [W_{\mu\nu\alpha\beta}(Q, k_1; \xi) + W_{\nu\mu\alpha\beta}(Q, k_1, \xi)] \varepsilon_{\lambda_\gamma}^{*\beta}(k_1) \varepsilon_{\lambda_G}^{*\mu\nu}(k_2) u_{\lambda_2}(p_1), \quad (25)$$

$$\mathcal{M}_c = \frac{\kappa g_f e}{2} \bar{v}_{\lambda_1}(p_2) [\gamma_\mu \eta_{\nu\alpha} + \gamma_\nu \eta_{\mu\alpha} - 2\eta_{\mu\nu} \gamma_\alpha] \times \varepsilon_{\lambda_\gamma}^{*\alpha}(k_1) \varepsilon_{\lambda_G}^{*\mu\nu}(k_2) u_{\lambda_2}(p_1). \quad (26)$$

Here,  $P \equiv (p_1 - k_1 - p_2) = (k_2 - 2p_2)$ ,  $Q \equiv -(p_1 + p_2)$  and  $K \equiv (p_1 + k_1 - p_2) = (2p_1 - k_2)$ . The fermions have spin states  $\lambda_1, \lambda_2 = \uparrow$  or  $\downarrow$ , and the photon has polarization states  $\lambda_\gamma = \pm 1$ . The graviton has polarization states  $\lambda_G = \pm 2, \pm 1$  and 0. We have chosen Feynman gauge with  $\xi = 1$ .

### III. RESULTS AND CONCLUSION

We first note that there are 40 combinations of outgoing helicities, with the corresponding incoming states of the spinors, with 16 each in helicity-2 and helicity-1 modes supplemented by 8 in helicity-0 modes. The helicity-2 modes correspond to polarizations of the massless graviton and have no bad small-mass behaviour. The helicity-0 mode exhibits the worst growth with decreasing graviton mass due to two factors of  $\varepsilon_0^\mu$ , where each factor grows as  $\mathcal{O}(1/M_G)$ . The total matrix element per-helicity is the sum of  $s$ ,  $t$ ,  $u$  and contact diagrams, which we, therefore, expand as a series in the mass of the graviton  $M_G$  to analyze if there are any divergences in the massless limit  $M_G \rightarrow 0$ ,

$$\mathcal{M}(s, \theta) = \sum_{\sigma \in \mathbb{Z}} M_G^\sigma \mathcal{M}(\theta). \quad (27)$$

<sup>7</sup>The matrix elements of above disagree with [1] in the  $u$ -channel only of Eq. (24). This can be a potential cause of the differing results.

Helicity-0 External Graviton: $(u, \bar{v}, \gamma, G) = (\uparrow, \uparrow, +1, 0)$	
Coefficient: $s (\kappa g_f e / 2\sqrt{3}) (m_f / M_G^2) \sin \theta$	
$\mathcal{M}_t$	$1 + \cos \theta \sqrt{1 - 4m_f^2/s}$
$\mathcal{M}_u$	$1 - \cos \theta \sqrt{1 - 4m_f^2/s}$
$\mathcal{M}_s$	-2
$\mathcal{M}_c$	0
$\sum \mathcal{M}$	0

TABLE I. The cancellations for a helicity-0 external graviton are presented. Note that  $\mathcal{M}_{t,u,s,c}$  represent the matrix element contributions for the diagrams depicted in Fig. 1

The entire matrix element for these diagrams are non-trivial, and thus Mathematica [23] was employed to compute the matrix element for each polarization symbolically. We also observe that several polarization combinations vanish simply by helicity conservation and selection rules, as tabulated in the supplementary materials.

Suppose that we choose some polarization state to investigate and interrogate the results from each Feynman diagram to determine the origin of the divergence. The leading divergent terms for the longitudinal polarization mode  $(u, \bar{v}, \gamma, G) = (\uparrow, \uparrow, +1, 0)$ , are demonstrated in Table I for the  $s$ ,  $t$ ,  $u$  and contact diagrams. We notice that while each of the  $s$ ,  $t$ ,  $u$  diagrams grow proportional to  $(m_f / M_G^2)$ , as expected from power counting arguments, the sum vanishes identically, leading to regular behaviour in the limit as  $M_G \rightarrow 0$ .

Scanning through every possible combination of the helicities, we find that the divergences in each channel exactly cancel when all channels are summed<sup>8</sup>. Therefore, the leading order term in the limit as  $M_G \rightarrow 0$  for all polarization combinations is a constant, including the scalar, vector and longitudinal polarizations of the graviton. Thus, no divergences persists once all diagrams are summed and hence,  $\sigma \geq 0$  in Eq. (27).

Squaring the amplitude we find no divergences in the limit as the graviton becomes massless  $M_G \rightarrow 0$ . The leading order in the limit is a constant term with respect to the graviton mass  $M_G$ ,

$$\lim_{M_G \rightarrow 0} |\mathcal{M}(s, \theta)|^2 = \mathcal{O}(M_G^0). \quad (28)$$

Considering now the high energy limit with a finite graviton mass  $M_G$ , the leading high energy contribution

to the matrix element for the helicity-0 modes is proportional to the fermion mass and is given by<sup>9</sup>,

$$\lim_{s \rightarrow \infty} \sum_{\lambda_G=0} |\mathcal{M}(s, \theta)| = \frac{4\kappa g_f e}{\sqrt{3}} m_f \csc \theta + \mathcal{O}(s^{-1}). \quad (29)$$

The series expansion in the high energy limit  $\sqrt{s} \rightarrow \infty$  is a physically interesting one. For example, we observe no anomalous behaviour in the high energy limit for the unpolarized process<sup>10</sup>,

$$\begin{aligned} \lim_{s \rightarrow \infty} \sum_{\text{all spins}} |\mathcal{M}(s, \theta)|^2 = & \frac{(\kappa g_f e)^2}{6} \left\{ 6s [3 + \cos(2\theta)] \right. \\ & + \left[ 27M_G^2 - 14m_f^2 - 6 [M_G^2 + 12m_f^2] \cos(2\theta) \right. \\ & \left. \left. + 3 [M_G^2 + 2m_f^2] \cos(4\theta) \right] \csc^2 \theta + \mathcal{O}(s^{-1}) \right\}. \end{aligned} \quad (30)$$

We next attempt to understand if there are underlying symmetry arguments that enforce the cancellation in terms proportional to powers of  $1/M_G$ . Pathologies in massive gravity theories come primarily from internal propagators [9]. Since we do not have them at tree-level for the process of interest, it is interesting to contemplate whether some QED-like Ward identity might effectively survive in this situation. The inclusion of an external graviton source in QED does not alter the global  $U(1)$  symmetry and so a conserved current will result. It seems reasonable to anticipate that an effective QED Ward identity might emerge in a careful treatment<sup>11</sup>, but an attempt at a formal proof of this is left for future work. We have directly verified for our amplitudes that we do have an effective Ward identity operating since we find

$$k_1^\alpha \mathcal{M}_\alpha = 0, \quad (31)$$

where the quantity  $\mathcal{M}_\alpha$  is defined such that  $\mathcal{M} \equiv \mathcal{M}_{\mu\nu\alpha} \varepsilon^\alpha(k_1) \varepsilon^{\mu\nu}(k_2) = \mathcal{M}_\alpha \varepsilon^\alpha(k_1)$ . This ensures that all contributions that grow as powers of  $1/M_G$  in individual diagrams cancel out for any given process.

While we have only explicitly calculated for the case of  $f\bar{f} \rightarrow G\gamma$  the above results will also apply to other tree-level amplitudes related by crossing symmetry such as  $\gamma\bar{f} \rightarrow Gf$ ,  $Gf \rightarrow \gamma\bar{f}$ ,  $\gamma\bar{f} \rightarrow G\bar{f}$ ,  $f \rightarrow fG\gamma$  and so on.

The above results will also survive at tree-level when a gluon replaces the photon in the external leg for any of these processes, where the only difference will be the replacement of the electromagnetic coupling by the strong

<sup>8</sup>It is reasonable to question if this result also holds when the amplitude is squared. The Supplementary Material shows that L'Hôpital's rule holds for arbitrary powers and complex numbers. Therefore, if the matrix element is regular in the limit as  $M_G \rightarrow 0$ , the matrix element squared will also be regular in the same limit by L'Hôpital's rule.

<sup>9</sup>Similar cancellations occur for helicity-1 modes and is documented in the supplementary materials.

<sup>10</sup>In [22], the cross-section for  $f\bar{f} \rightarrow \gamma G_{KKm}$  in the  $m_f \rightarrow 0$  limit is provided, showing no enhancements proportional to  $1/M_{KK}^2$ . We agree with this result.

<sup>11</sup>For a derivation of Ward identity, see for example [24].

coupling constant. For example, we note that this breaks down when considering two massive graviton emissions, i.e., a process like  $f\bar{f} \rightarrow GG$ , due to the presence of an  $s$ -channel diagram with a massive graviton in the internal propagator. In this case, there is no mechanism by which this cancellation can take place for a theory of massive gravity [25]. However, in KK theories, a sum over all modes in the internal propagator restores the unitarity due to higher dimensional diffeomorphism invariance.

Therefore, we have demonstrated no enhancements in the limit as  $M_G \rightarrow 0$  in the matrix elements of massive graviton-photon scattering with initial fermion states, regardless of whether the fermion is massive or not, contrary to claims in [1]. Therefore, the dark matter scenario for which the authors claim large enhancements in the velocity-averaged cross-section appears inconsistent with our calculation. In passing, we note that in [12], Section 3.4 seems to claim that there may be an enhancement at the cross-section level for the process

with a radion external state in a full KK theory for a finite fermion mass. It would be a worthwhile exercise to re-evaluate this result given our findings here, but it is beyond the scope of this paper.

**Acknowledgements** JAG acknowledges the support he has received for his research through the provision of an Australian Government Research Training Program Scholarship. Support for this work was provided by the University of Adelaide and the Australian Research Council through the Centre of Excellence for Dark Matter Particle Physics (CE200100008). DS acknowledges the Mainz Institute of Theoretical Physics workshop ‘Towards the Next Fundamental Scale of Nature: New Approaches in Particle Physics and Cosmology’, where this project originated. DS and JAG thank Seung J. Lee and Giacomo Cacciapaglia for illuminating conversations. DS also thanks R. Sekhar Chivukula, Xing Wang and Kirtimaan Mohan for the discussions.

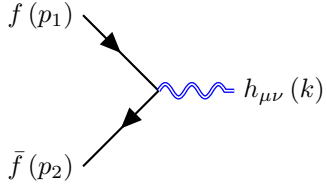
- 
- [1] H. Cai, G. Cacciapaglia, and S. J. Lee, “Massive gravitons as feebly interacting dark matter candidates,” *Phys. Rev. Lett.* **128** (Feb, 2022) 081806, <https://link.aps.org/doi/10.1103/PhysRevLett.128.081806>.
- [2] M. Garny, M. Sandora, and M. S. Sloth, “Planckian Interacting Massive Particles as Dark Matter,” *Phys. Rev. Lett.* **116** no. 10, (2016) 101302, [arXiv:1511.03278 \[hep-ph\]](https://arxiv.org/abs/1511.03278).
- [3] M. G. Folgado, A. Donini, and N. Rius, “Gravity-mediated Scalar Dark Matter in Warped Extra-Dimensions,” [arXiv:1907.04340 \[hep-ph\]](https://arxiv.org/abs/1907.04340). [Erratum: *JHEP* 02, 129 (2022)].
- [4] T. D. Rueter, T. G. Rizzo, and J. L. Hewett, “Gravity-Mediated Dark Matter Annihilation in the Randall-Sundrum Model,” *JHEP* **10** (2017) 094, [arXiv:1706.07540 \[hep-ph\]](https://arxiv.org/abs/1706.07540).
- [5] S. Kraml, U. Laa, K. Mawatari, and K. Yamashita, “Simplified dark matter models with a spin-2 mediator at the LHC,” *Eur. Phys. J. C* **77** no. 5, (2017) 326, [arXiv:1701.07008 \[hep-ph\]](https://arxiv.org/abs/1701.07008).
- [6] H. van Dam and M. J. G. Veltman, “Massive and massless Yang-Mills and gravitational fields,” *Nucl. Phys. B* **22** (1970) 397–411.
- [7] V. I. Zakharov, “Linearized gravitation theory and the graviton mass,” *JETP Lett.* **12** (1970) 312.
- [8] M. Fierz and W. Pauli, “On relativistic wave equations for particles of arbitrary spin in an electromagnetic field,” *Proc. Roy. Soc. Lond. A* **173** (1939) 211–232.
- [9] C. de Rham, G. Gabadadze, and A. J. Tolley, “Resummation of Massive Gravity,” *Phys. Rev. Lett.* **106** (2011) 231101, [arXiv:1011.1232 \[hep-th\]](https://arxiv.org/abs/1011.1232).
- [10] C. de Rham, “Massive Gravity,” *Living Rev. Rel.* **17** (2014) 7, [arXiv:1401.4173 \[hep-th\]](https://arxiv.org/abs/1401.4173).
- [11] K. Hinterbichler, “Theoretical Aspects of Massive Gravity,” *Rev. Mod. Phys.* **84** (2012) 671–710, [arXiv:1105.3735 \[hep-th\]](https://arxiv.org/abs/1105.3735).
- [12] T. Han, J. D. Lykken, and R.-J. Zhang, “Kaluza-klein states from large extra dimensions,” *Physical Review D* **59** no. 10, (Mar, 1999) . <https://doi.org/10.1103%2Fphysrevd.59.105006>.
- [13] L. Randall and R. Sundrum, “A Large mass hierarchy from a small extra dimension,” *Phys. Rev. Lett.* **83** (1999) 3370–3373, [arXiv:hep-ph/9905221](https://arxiv.org/abs/hep-ph/9905221).
- [14] L. Randall and R. Sundrum, “An Alternative to compactification,” *Phys. Rev. Lett.* **83** (1999) 4690–4693, [arXiv:hep-th/9906064](https://arxiv.org/abs/hep-th/9906064).
- [15] “Massive spin-2 scattering amplitudes in extra-dimensional theories,” *Physical review. D* **101** no. 7, (2020) 1–.
- [16] R. Sekhar Chivukula, D. Foren, K. A. Mohan, D. Sengupta, and E. H. Simmons, “Sum Rules for Massive Spin-2 Kaluza-Klein Elastic Scattering Amplitudes,” *Phys. Rev. D* **100** no. 11, (2019) 115033, [arXiv:1910.06159 \[hep-ph\]](https://arxiv.org/abs/1910.06159).
- [17] R. Sekhar Chivukula, D. Foren, K. A. Mohan, D. Sengupta, and E. H. Simmons, “Scattering amplitudes of massive spin-2 Kaluza-Klein states grow only as  $\mathcal{O}(s)$ ,” *Phys. Rev. D* **101** no. 5, (2020) 055013, [arXiv:1906.11098 \[hep-ph\]](https://arxiv.org/abs/1906.11098).
- [18] R. S. Chivukula, D. Foren, K. A. Mohan, D. Sengupta, and E. H. Simmons, “Spin-2 Kaluza-Klein scattering in a stabilized warped background,” *Phys. Rev. D* **107** no. 3, (2023) 035015, [arXiv:2206.10628 \[hep-ph\]](https://arxiv.org/abs/2206.10628).
- [19] R. S. Chivukula, D. Foren, K. A. Mohan, D. Sengupta, and E. H. Simmons, “Spin-2 Kaluza-Klein mode scattering in models with a massive radion,” *Phys. Rev. D* **103** no. 9, (2021) 095024, [arXiv:2104.08169 \[hep-ph\]](https://arxiv.org/abs/2104.08169).
- [20] A. de Giorgi and S. Vogl, “Unitarity in KK-graviton production: A case study in warped extra-dimensions,” *JHEP* **04** (2021) 143, [arXiv:2012.09672 \[hep-ph\]](https://arxiv.org/abs/2012.09672).
- [21] N. E. J. Bjerrum-Bohr, B. R. Holstein, L. Planté, and P. Vanhove, “Graviton-Photon Scattering,”

- Phys. Rev. D **91** no. 6, (2015) 064008,  
[arXiv:1410.4148 \[gr-qc\]](https://arxiv.org/abs/1410.4148).
- [22] G. F. Giudice, R. Rattazzi, and J. D. Wells, “Quantum gravity and extra dimensions at high-energy colliders,” Nuclear Physics B **544** no. 1-2, (Apr, 1999) 3–38.  
<https://doi.org/10.1016%2Fs0550-3213%2899%2900044-9>.
- [23] W. R. Inc., “Mathematica, Version 13.2.”  
<https://www.wolfram.com/mathematica>. Champaign, IL, 2022.
- [24] A. G. Williams, Introduction to Quantum Field Theory: Classical Mechanics to Gauge Field Theories. Cambridge University Press, 2022.
- [25] A. Falkowski and G. Isabella, “Matter coupling in massive gravity,” JHEP **04** (2020) 014,  
[arXiv:2001.06800 \[hep-th\]](https://arxiv.org/abs/2001.06800).

## Appendix A: Supplementary Material

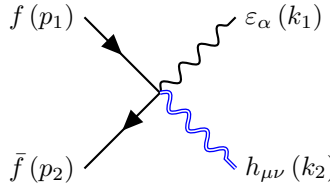
### 1. Feynman Rules

The Feynman rules for the various vertices are demonstrated below and agree with [12]. In these diagrams, momentum flows left to right:



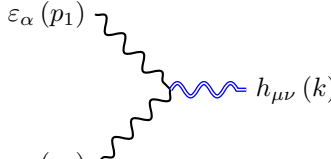
(A1)

$$= -\frac{i\kappa}{4} \left[ (p_1 - p_2)_\mu \gamma_\nu + (p_1 - p_2)_\nu \gamma_\mu - 2\eta_{\mu\nu} (\not{p}_1 - \not{p}_2 - 2m_f) \right].$$



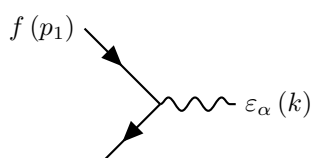
(A2)

$$= \frac{i\kappa g_f e}{2} \left[ \gamma_\mu \eta_{\nu\alpha} + \gamma_\nu \eta_{\mu\alpha} - 2\eta_{\mu\nu} \gamma_\alpha \right].$$



(A3)

$$= -i\kappa [W_{\mu\nu\alpha\beta}(-p_1, -p_2, \xi) + W_{\nu\mu\alpha\beta}(-p_1, -p_2, \xi)].$$



(A4)

$$= -ig_f e \gamma_\alpha.$$

### 2. Limit Raised to a Power Proof

Using L'Hôpital's rule, we can show that L'Hôpital's rule holds when the limit is raised to a power. Suppose

that  $\lim_{x \rightarrow 0} f(x) = 0 = \lim_{x \rightarrow 0} g(x)$ .

$$\begin{aligned} & \lim_{x \rightarrow 0} \frac{[f(x)]^n}{[g(x)]^n} \\ &= \lim_{x \rightarrow 0} \frac{n [f(x)]^{n-1} f'(x)}{n [g(x)]^{n-1} g'(x)} \\ &= \lim_{x \rightarrow 0} \frac{n(n-1) [f(x)]^{n-2} [f'(x)]^2 + n [f(x)]^{n-1} f''(x)}{n(n-1) [g(x)]^{n-2} [g'(x)]^2 + n [g(x)]^{n-1} g''(x)}. \end{aligned} \quad (\text{A5})$$

The above result is still in the form of a 0/0 limit for  $n > 2$ . Note that provided  $f'(0)$  and  $g'(0) \neq 0$  then as  $x \rightarrow 0$  the left hand term completely dominates for any  $n > 0$  in both the numerator and the denominator. So the second term in each can be discarded. To achieve a regular result, we require the numerator and the denominator to both have a term that appears as  $[f(x)]^0$  and  $[g(x)]^0$ . Repeating L'Hôpital's rule  $n$  times, we find that L'Hôpital's rule holds for any arbitrary powers in the form

$$\begin{aligned} & \lim_{x \rightarrow 0} \frac{[f(x)]^n}{[g(x)]^n} = \lim_{x \rightarrow 0} \frac{n(n-1) [f(x)]^{n-2} [f'(x)]^2 + \dots}{n(n-1) [g(x)]^{n-2} [g'(x)]^2 + \dots} \\ &= \lim_{x \rightarrow 0} \frac{n(n-1)(n-2) [f(x)]^{n-3} [f'(x)]^3 + \dots}{n(n-1)(n-2) [g(x)]^{n-3} [g'(x)]^3 + \dots} \\ &= \dots = \lim_{x \rightarrow 0} \frac{n! [f'(x)]^n + \dots}{n! [g'(x)]^n + \dots} = \lim_{x \rightarrow 0} \frac{[f'(x)]^n}{[g'(x)]^n}. \end{aligned} \quad (\text{A6})$$

For  $n = 2$  we have for example,

$$\lim_{x \rightarrow 0} \frac{[f(x)]^2}{[g(x)]^2} = \lim_{x \rightarrow 0} \frac{[f'(x)]^2}{[g'(x)]^2}. \quad (\text{A7})$$

Suppose  $f(x)$  is a complex-valued function and  $g(x)$  is a real-valued function. The complex-valued function  $f(x)$  can be decomposed as a sum of two real-valued functions  $a(x)$  and  $b(x)$  such that  $f(x) = a(x) + ib(x)$ . Note that to preserve the existing limits assumed on  $f(x)$  and  $g(x)$ , we assume that  $\lim_{x \rightarrow 0} a(x) = 0 = \lim_{x \rightarrow 0} b(x)$ . Taking the limit as  $x \rightarrow 0$  of the modulus squared of  $f(x)/g(x)$ , we find that L'Hôpital's rule holds as an extension of the above result,

$$\begin{aligned} & \lim_{x \rightarrow 0} \frac{|f(x)|^2}{|g(x)|^2} = \lim_{x \rightarrow 0} \frac{[a(x)]^2 + [b(x)]^2}{[g(x)]^2} \\ &= \lim_{x \rightarrow 0} \frac{[a'(x)]^2 + [b'(x)]^2}{[g'(x)]^2} = \lim_{x \rightarrow 0} \frac{|f'(x)|^2}{|g'(x)|^2}. \end{aligned} \quad (\text{A8})$$

This is all we need here, but generalizations to allow  $g(x) = c(x) + id(x)$  as well and to allow for only one of  $a(x)$  and  $b(x)$  and/or only one of  $c(x)$  and  $d(x)$  to vanish as  $x \rightarrow 0$  are straightforward.

### 3. Cancellations in the Helicity-1 Modes

A limit-taking process is performed in Mathematica on each channel resulting from the different Feynman diagrams, and we find a definite divergence in the limit

Vector Polarization: $(u, \bar{v}, \gamma, G) = (\uparrow, \uparrow, +1, +1)$	
Coefficients of: $(\kappa g_f e) \sqrt{s/2} (m_f/M_G)$	
$\mathcal{M}_t$	$\sin^2 \theta \sqrt{1 - 4m_f^2/s} + (1 - \cos \theta)/2$
$\mathcal{M}_u$	$-\sin^2 \theta \sqrt{1 - 4m_f^2/s} - (1 + \cos \theta)/2$
$\mathcal{M}_s$	$2 \cos \theta$
$\mathcal{M}_c$	$-\cos \theta$
$\sum \mathcal{M}$	0

TABLE II. The cancellations for a helicity-1 external graviton are presented. Note that  $\mathcal{M}_{t,u,s,c}$  represent the matrix element contributions for the diagrams depicted in Fig. 1

as  $M_G \rightarrow 0$  for individual diagrams. The leading divergent terms for the polarization mode  $(u, \bar{v}, \gamma, G) = (\uparrow, \uparrow, +1, +1)$  are provided in Table II.

We show that cancellations in the matrix element in the helicity-1 mode are identical to that of the helicity-0 mode. As before, the divergent pieces in the  $t$  and  $u$  channels are exactly cancelled by the divergent pieces in the  $s$ -channel and contact term, such that the limit as  $M_G \rightarrow 0$  is regular. As we scan through all polarization combinations, we find that the same pattern follows for each polarization state for the vector modes of the graviton.

#### 4. Table of Components for Polarizations

A series of tables containing the leading divergence piece of each polarization combination for the individual diagrams are shown below. For a box in the tables below containing the number  $j$ , we mean that the leading order term as  $M_G \rightarrow 0$  for the matrix element of graviton polarization  $\lambda_G$  and photon polarization  $\gamma$  is proportional to  $(M_G)^j$ . The choice of fermion spins were inconsequential to the result, and so the number represents the leading divergent piece for all choices of fermion spins.

In Table III, we highlight that each polarization combination grows as expected by power counting. In Tables

IV and V, we find that some polarization combinations vanish identically. We expect the  $t$  and  $u$ -channel divergences to cancel directly in these instances. Interestingly, the contact term is regular in the longitudinal mode but not the vector mode. The divergent contribution here is proportional to  $\varepsilon_0(k_2) \cdot \varepsilon_{\lambda_\gamma}(k_1) = 0$ , which evaluates to zero as they are orthogonal in the centre-of-momentum frame.

$\mathcal{M}_{t,u} \sim \mathcal{O}(M_G)$						
	$\lambda_G$					
	-2	-1	0	+1	+2	
$\gamma$	+1	0	-1	-2	-1	0
	-1	0	-1	-2	-1	0

TABLE III.  $t$ -Channel and  $u$ -Channel Divergence Breakdown

$\mathcal{M}_s \sim \mathcal{O}(M_G)$						
	$\lambda_G$					
	-2	-1	0	+1	+2	
$\gamma$	+1	0	0	-2	-1	0
	-1	0	-1	-2	0	0

TABLE IV.  $s$ -Channel Divergence Breakdown

$\mathcal{M}_c \sim \mathcal{O}(M_G)$						
	$\lambda_G$					
	-2	-1	0	+1	+2	
$\gamma$	+1	0	0	0	-1	0
	-1	0	-1	0	0	0

TABLE V. Contact Term Divergence Breakdown